Differ Equ Dyn Syst (July 2016) 24(3):281–303
DOI 10.1007/s12591-014-0234-6

ORIGINAL RESEARCH

The Effects of Latent Infection on the Dynamics of HIV

Stephen Pankavich

Published online: 21 January 2015

Abstract One way in which the human immunodeficiency virus (HIV-1) replicates within a host is by infecting activated CD4+ T-cells, which then produce additional copies of the virus. Even with the introduction of antiretroviral drug therapy, which has been very successful over the past decade, a large obstacle to the complete eradication of the virus is the presence of viral reservoirs in the form of latently infected CD4+ T-cells. We consider a model of HIV infection that describes T-cell and viral interactions, as well as, the production and activation of latently infected T-cells. Upon determining equilibrium states of the latent cell model, the local and global asymptotic behavior of solutions is examined, and the basic reproduction number of the system is computed to be strictly less than that of the corresponding three-component model, which omits the effects of latent infection. In particular, this implies that a wider variety of parameter values will lead to viral eradication as $t \to \infty$ due to the appearance of latent CD4+ T-cells. With this realization we discuss possible alternative notions for eradication and persistence of infection other than traditional dynamical tools. These results are further illustrated by a number of numerical simulations.

Keywords HIV-1 · Mathematical model · Latently infected T-cells · Antiretroviral therapy · Global asymptotic stability

Introduction

The majority of cells infected with the human immunodeficiency virus (HIV-1) are activated CD4+ T-cells. Once infected, these cells produce additional copies of virus, thereby prolonging the infection. Upon detecting such an infection, the immune system mounts a complex adaptive response, controlling the virus population to a limited extent. Further control is available in the form of antiretroviral drugs, such as reverse transcriptase inhibitors (RTIs) and protease inhibitors (PIs) [17]. If such drugs are taken with sufficient frequency, the virus

S. Pankavich (✉)
Department of Applied Mathematics and Statistics, Colorado School of Mines, Golden, CO 80401, USA
e-mail: pankavic@mines.edu

population is largely limited and remains below the level of detection [6]. However, antiretroviral therapy (ART) cannot fully eradicate the virus, as viral rebound occurs once therapy is interrupted [1,12] A number of factors have been proposed to explain this viral rebound. Most notably, it has been suggested that HIV lay dormant within a number of reservoirs. Primary among these reservoirs are latently infected CD4 + T-cells [2]. Though latently infected T-cells exist in the body with a much lower frequency than susceptible CD4 + T-cells, the reservoir appears to decay very slowly, with a half-life measured between 6 and 48 months [27]. Although infected, these cells do not produce new virions until activated, thus potentially providing a longer-lived hiding place where the virus may evade control by either the immune system or antiretroviral treatment [2]. Consequently, in this paper, we analyze a mathematical model that includes latent infection and examine the control of infection by ART. We also assume that such latent T-cells exist significantly longer than productively infected CD4 + T-cells. Ultimately, we will show that a mathematical analysis of the most basic latent model demonstrates that the inclusion of such cells increases the likelihood for viral clearance only as $t \to \infty$, under the traditional approach of analyzing the basic reproduction number and the associated stability of equilibria. While this will seem intuitive from a modeling perspective, as described later, it also appears contradictory to the widely-held notion that latently infected T-cells are an important mechanism for the inability of ART to eradicate an established infection. What this really implies is that standard mathematical tools are insufficient to realistically describe the dynamics of HIV when latent cells are considered. Instead, one must focus on the rate of decay of the infection, which is significantly slowed by the latent T-cell population.

A number of authors have studied the biological aspects of mathematical models concerning HIV dynamics that consider latently infected cells. Notably, Callaway and Perelson [4] studied low-level viremia, Rong and Perelson [29] modeled viral blips and showed that a latent reservoir could produce viral transients when activated by infection, while Sedaghat et al. [32] employed a simple model for the dynamics of the latent reservoir to show that its stability was unlikely to stem from ongoing replication during ART. In each of these studies, a reduced or linearized mathematical analysis was performed, but the nonlinear behavior of the associated model was not fully elucidated. In the current study, we describe latently infected cells using a separate compartment, as did these authors, by assuming that a proportion of newly-infected cells become latently infected upon contact with the virus, but that they are not productively infected until they leave the latent state, which occurs at a rate α proportionate to the size of the latent cell population. We note that the effects of viral mutation, which may continuously change model and parameter values, and the possible spatial dependence of parameters are ignored. Using this model, we study the influence of the latent reservoir on the persistence of HIV infection and viral rebound. Our results provide a new perspective on the methods of mathematical and stability analysis for viral and latent reservoir persistence.

The paper proceeds as follows. In the next section, we will review some known results concerning the standard three-component model of HIV dynamics. After this, we introduce an additional population representing latently infected CD4+ T-cells, and study the effects that these cells have on the structure and behavior of the long-time dynamics of the model. Next, we discuss the ramifications of our results and, in particular, the need to construct more precise notions of viral eradication and persistence. The penultimate section contains proofs of the theorems contained within previous sections. In the final section, we conclude with a discussion of our results.

The Three-Component Model

In general, the modeling of HIV dynamics in vivo is complicated by the appearance of spatial inhomogeneities, which can arise from various reservoirs, such as those occurring within lymphatic tissues [19,26]. Even when such inhomogeneities are ignored, however, these systems are often described to a sufficient degree by systems of ordinary differential equations that include no spatial dependence. We begin by considering a three-component model for the evolution of within-host HIV, that does not include spatial fluctuations or effects due to long-lived infected or latently infected cells. This model has been widely-accepted as a descriptive representation for the basic dynamics of HIV [3,24,37]. It represents the populations of three components in a fixed volume at a given time t: $T(t)$, the number of CD4+ T-cells that are susceptible to HIV-1 infection, $I(t)$ the number of infected T-cells that are actively producing virus particles, and $V(t)$ the number of free virions. These quantities approximately satisfy the system of ordinary differential equations

$$\begin{cases} \dfrac{dT}{dt} = \lambda - d_T T - kTV, \\ \dfrac{dI}{dt} = kTV - d_I I, \\ \dfrac{dV}{dt} = N d_I I - d_V V. \end{cases} \tag{1}$$

Here λ is the recruitment rate of susceptible T-cells and d_T is their mortality rate. The constant k represents the rate of infection, which is included within a bilinear mass action term, while d_I is the death rate of productively infected cells and d_V is the clearance rate of free virus. The parameter N is the burst size, i.e. the total number of virions produced by an infected cell during its life span.

The behavior of solutions to these equations has previously been analyzed in great detail [3,34,37,38]. In particular, it is known that exactly two steady states exist, which we will write in the form (T, I, V), namely an uninfected equilibrium

$$E_{NI} : \left(\frac{\lambda}{d_T}, 0, 0\right)$$

and an infected equilibrium

$$E_I : \left(\frac{\lambda}{d_T R_0}, \frac{d_T d_V}{kNd_I}(R_0 - 1), \frac{d_T}{k}(R_0 - 1)\right),$$

where

$$R_0 = \frac{\lambda k N}{d_V d_T}$$

is the basic reproduction number of the system. The stability properties of these steady states are also well-known and depend only upon the single parameter R_0. In particular, one can study the linearized analogue of (1) and prove the local asymptotic stability of E_{NI} if $R_0 \leq 1$ and the local asymptotic stability of E_I if $R_0 > 1$ [38]. This result effectively states that for starting values of the populations which are close enough to the given equilibria, the solutions will tend to the respective equilibrium point as $t \to \infty$. Additionally, the global asymptotic stability of these equilibria is known. In [20] it was shown that initial populations are irrelevant in determining the long term dynamics of the solution. More specifically, if $R_0 \leq 1$, then for any initial population of uninfected cells, infected cells, and virions the

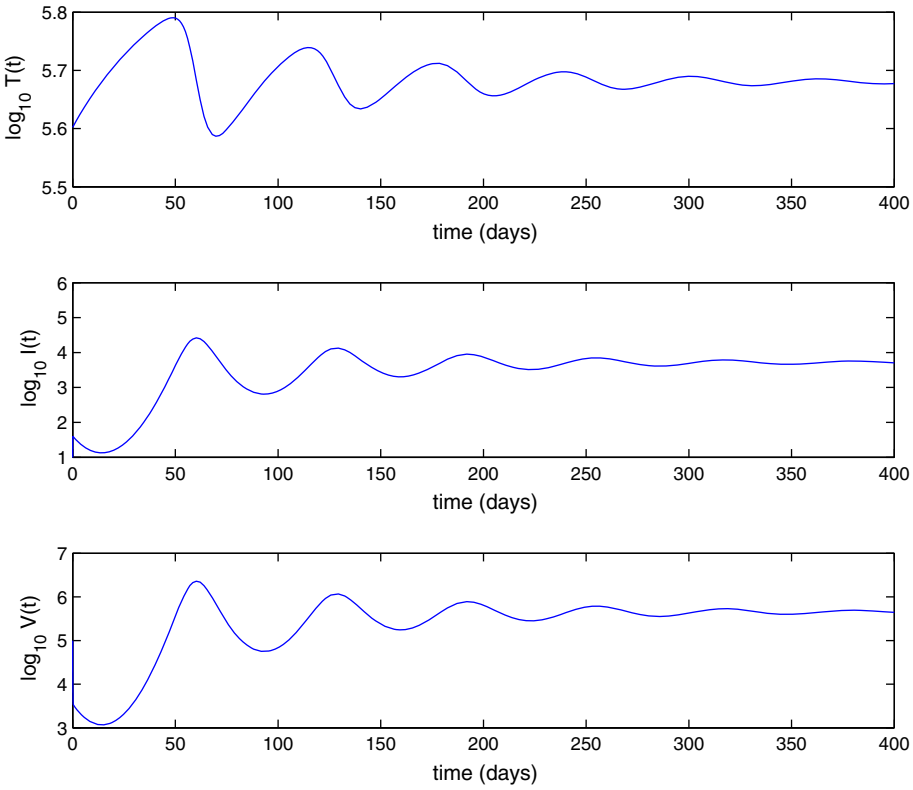

Fig. 1 A representative solution of (1) with parameter values stated in Table 1. The initial T-cell population is $T(0) = 4 \times 10^5$, while the initial viral load is $V(0) = 10^5$, and $I(0) = 0$ as in [4]. In this example, the system tends to the infected equilibrium as $t \to \infty$ because $R_0 = 2.087$

solutions of (1) tend to E_{NI} as $t \to \infty$. Contrastingly, if $R_0 > 1$ the same result holds for the infected equilibrium E_I. Figure 1 displays a representative graph of solutions for which $R_0 > 1$ and hence viral infection persists.

Inclusion of Latently-Infected Cells

Though (1) describes the basic mechanisms which account for the spread of HIV, it lacks the ability to describe the latent stage of a specific subpopulation of infected T-cells. Many studies [7,9,10] have determined that upon infection and transcription of viral RNA into cell DNA, a fraction of CD4+ T-cells fail to actively produce virus until they are activated, possibly years after their initial infection. Such cells may possess a much longer lifespan than their counterparts, and are termed latently infected. Upon activation, latently infected cells do become actively productive, and hence begin to increase the viral load through viral replication. A basic model of latent cell activation was initially developed to examine cell populations that contribute to the viral decline that occurs after administration of antiretroviral therapy [23]. However, within [23] and other articles by related authors [24,29,30], the mathematical analysis of the model is performed under a number of limiting assumptions,

including a constant background population of susceptible T-cells and perfect efficacy of anti-retroviral drugs. Thus, we focus on determining (and proving) the resulting nonlinear dynamics without these assumptions.

As for (1) we consider a model describing T-cells that may be susceptible or infected. In addition, we let $L(t)$ represent the new population of latently infected T-cells that cannot produce virions at time t but begin to do so once they are activated by recall antigens. With this addition, the previously described three-component model now contains four components and is given by

$$\begin{cases} \dfrac{dT}{dt} = \lambda - d_T T - kTV, \\ \dfrac{dI}{dt} = (1-p)kTV + \alpha L - d_I I, \\ \dfrac{dL}{dt} = pkTV - \alpha L - d_L L, \\ \dfrac{dV}{dt} = Nd_I I - d_V V. \end{cases} \tag{2}$$

Here, $p \in (0, 1)$ is the proportion of infections that lead to the production of a latently infected T-cell, rather than a productively infected T-cell, and α is the rate at which latently infected cells transition to become actively productive. Additionally, d_L is the rate at which latent cells are cleared from the system. Figure 2 displays a representative graph of solutions to (2). We note that the oscillations of T, I, and V seem quite damped in comparison to those of Fig. 1.

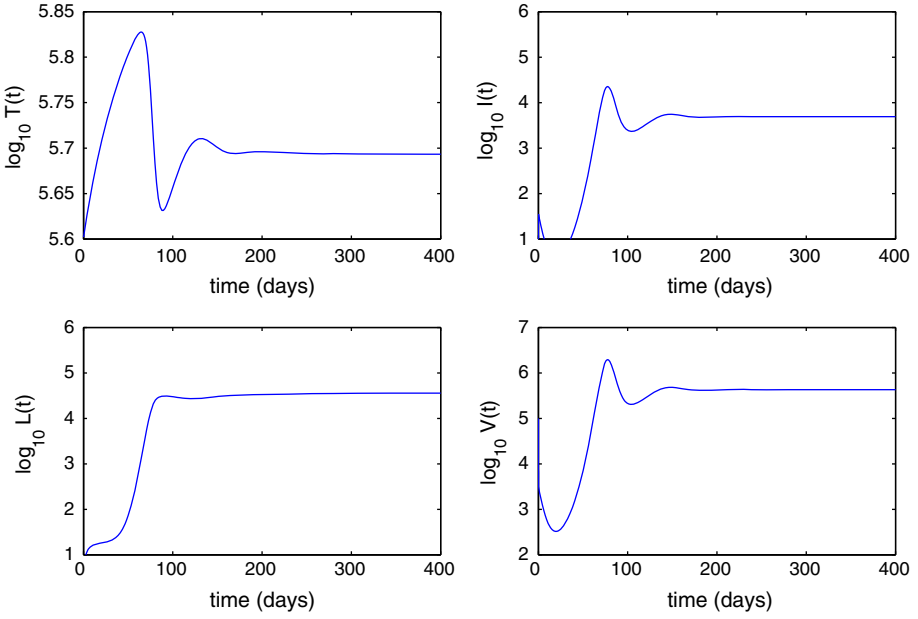

Fig. 2 A representative solution of (2) with parameters from Table 1. The initial values are $T(0) = 4 \times 10^5$, $V(0) = 10^5$, and $I(0) = 0$ as in [4], and $L(0) = 0$. In this example, the system tends to the infected equilibrium as $t \to \infty$ because $R_L = 2.027$. In comparison to Fig. 1, oscillations within the populations are strongly damped

Model Parameters

In this section and the previous one, we have adopted parameter values from other studies. A few of these parameters possess generally agreed upon values, including λ, d_T, d_I, and d_V. However, it should be noted that λ and d_T are typically estimated for healthy individuals, and thus may not be reliable estimates to describe HIV patients, especially those who experience impaired thymic function [18]. Obviously, there are many parameters, and these are summarized within Table 1, along with descriptions of the variables, their associated units, and references from which parameter values stem.

The parameter that displays the most uncertainty within the literature is the viral infectivity k which fluctuates by an order of magnitude from 2.4×10^{-8} ml/day [24,29] to 2.7×10^{-7} ml/day [36]. The value we utilize here is at the low end of this range and stems from [24]. Biologically relevant values of the in vivo burst size N are also somewhat uncertain. Estimates based on counting HIV-1 RNA molecules in an infected cell vary between hundreds and thousands [15,16,29], and estimates based on viral production have been as high as 5×10^4 [5,11]. Here, we choose $N = 2{,}000$ HIV-1 RNA/cell as reported in [16].

Parameters that stem specifically from (2) are generally not well-known. In particular, the activation rate α varies from study to study, but based on previous work [4,18], we use $\alpha = 0.01$ per day. Similarly, the removal rate of latently infected cells, d_L, has been discussed as anywhere from 10^{-3} per day [29] to 0.24 per day [36]. Hence, we chose a value with this range, namely $d_L = 4 \times 10^{-3}$ per day, as reported within [14]. The proportion p of cells which are categorized as latent upon becoming infected also differs throughout recent studies, ranging from 1.5×10^{-6} in [4] to 0.1 in [36]. In this case, we utilize the latter value so as to emphasize changes in (1) due to the latent cell population. Initial conditions of the proposed model are chosen to match clinically observed decay characteristics of the latent reservoir and the virus population. In particular, we utilize values similar to [4], namely $T(0) = 4 \times 10^5$,

Table 1 Variable and parameter values for (1) and (2)

Variable	Units	Description	Value	Reference
$T(t)$	Cells ml^{-1}	Susceptible CD4+ T-cells	–	–
$I(t)$	Cells ml^{-1}	Actively infected CD4+ T-cells	–	–
$L(t)$	Cells ml^{-1}	Latently infected CD4+ T-cells	–	–
$V(t)$	Virions ml^{-1}	Infectious virions	–	–
λ	ml^{-1} day^{-1}	Production rate of CD4+ T-cells	10^4	[4]
d_T	day^{-1}	Death rate of susceptible T cells	0.01	[21]
d_I	day^{-1}	Death rate of actively infected T cells	1	[22]
d_V	day^{-1}	Clearance rate of virions	23	[28]
k	ml day^{-1}	Rate of infection of susceptible cells	2.4×10^{-8}	[24]
N	–	Burst rate of actively infected T-cells	2,000	[16]
d_L	day^{-1}	Death rate of latent cells	4×10^{-3}	[14]
α	day^{-1}	Activation rate of latent cells	0.01	[4]
p	–	Proportion of latent infection	0.1	[36]
ϵ_{RT}	–	Efficacy of RT inhibitor	Varies	–
ϵ_{PI}	–	Efficacy of protease inhibitor	Varies	–

$I(0) = 0$, $L(0) = 0$, and $V(0) = 10^5$. Next, we analyze properties of solutions to (2) so as to compare their dynamics and large time behavior with solutions of (1).

Analysis and Properties of Solutions

As a first step, we can say with certainty that biologically reasonable values of the parameters give rise to positive populations assuming that at some earlier point (perhaps at the initial time) the populations possessed positive values.

Theorem 1 *Assume all constants in (2) are nonnegative and the initial values $T(0)$, $I(0)$, $L(0)$, and $V(0)$ are positive. Then, the solutions of (2), namely $T(t)$, $I(t)$, $L(t)$, and $V(t)$ exist, are unique, and remain bounded on the interval $[0, t^*]$ for any $t^* > 0$. Additionally, each function remains positive for any $t \geq 0$.*

Of course, the requirement of initial positivity is not completely necessary since we may translate or rescale the time variable to alter the initial time. Hence, what is necessary for the theorem to hold is that all populations must attain positive values at *some* time. This result provides some general validation for the model since it implies that negative population values cannot occur if one begins with biologically reasonable (i.e., positive) values.

Next, we proceed as for (1) and investigate equilibrium states of (2) and their stability properties. Solving the nonlinear system of algebraic equations

$$\begin{cases} 0 = \lambda - d_T T - kTV, \\ 0 = (1-p)kTV + \alpha L - d_I I, \\ 0 = pkTV - \alpha L - d_L L, \\ 0 = Nd_I I - d_V V. \end{cases} \tag{3}$$

for the unknown constants T, I, L, and V in terms of the parameters λ, k, p, α, N, d_T, d_I, d_L, and d_V, we find the existence of exactly two steady states.

Writing these in the form (T, I, L, V), they are

$$E_{NI} : \left(\frac{\lambda}{d_T}, 0, 0, 0\right),$$
$$E_I : \left(\frac{\lambda}{d_T R_L}, \frac{d_T d_V}{kNd_I}(R_L - 1), \frac{p\lambda}{R_L(d_L + \alpha)}(R_L - 1), \frac{d_T}{k}(R_L - 1)\right).$$

As before, we denote the uninfected equilibrium by E_{NI} and the infective equilibrium by E_I. Notice that the limiting values of T, I, and V for the infective state are of the same form as those of (1), with R_L replacing the role of R_0. Additionally, we see that if $R_L = 1$, then the equilibria coincide, and if $R_L < 1$, then the infected equilibrium corresponds to negative values which, in view of Theorem 1, cannot be obtained from biologically relevant initial data.

By studying the linearized version of the system, we may examine the local stability of these equilibria and find that their behavior mimics that of (1).

Theorem 2 *If $R_L \leq 1$, then the uninfected equilibrium is locally asymptotically stable. If $R_L > 1$ then the uninfected equilibrium is an unstable saddle point, and the infected equilibrium is locally asymptotically stable.*

Therefore, if $R_L \leq 1$ and population values begin within a sufficiently close distance of E_{NI}, then they will tend to E_{NI} as $t \to \infty$. Contrastingly, if $R_L > 1$ and initial populations are

sufficiently close to E_I, they will tend to E_I in the long run. Theorem 2 also emphasizes the crucial feature that equilibria are not stable simultaneously, that is, bistability of E_{NI} and E_I does not occur. Furthermore, it expresses that the qualitative behavior of system (2) changes exactly when R_L transitions from less than one to greater than one, and hence a bifurcation occurs at $R_L = 1$.

The final theorem of the section demonstrates the stronger result that initial values of these populations have no effect on their long term ($t \to \infty$) limiting values.

Theorem 3 *If $R_L \leq 1$, then the uninfected equilibrium is globally asymptotically stable. If $R_L > 1$, then the infected equilibrium is globally asymptotically stable.*

This analysis reveals one very important fact about the overall system: the end states of populations are only dependent on the value of R_L, and not any other parameter or initial value. If R_L is greater than one, then the system tends to E_I, an end state with a non-zero population of infected cells and virions, but if R_L is less than one, then the final equilibrium is E_{NI}, which contains neither virions nor infected T-cells.

The most important feature of these results is the explicit formula for R_L, which can be related exactly to the basic reproductive number of the three-component model (1). In order to investigate the differences between the two reproductive ratios, we define the quantity

$$Q := \frac{R_L}{R_0} = \frac{(1-p)d_L + \alpha}{d_L + \alpha}. \tag{4}$$

Notice that Q depends only upon the three new parameters included within (2), namely the activation ratio α, proportion of cells which become latent upon infection p, and the death rate of latent cells d_L. Additionally, if the proportion p of infections which produce latently infected T-cells is identically zero, then $R_L = R_0$. However, since we consider $p \in (0, 1)$ we find

$$Q < \frac{d_L + \alpha}{d_L + \alpha} = 1$$

and the relationship

$$R_L < R_0$$

follows directly. Thus, the reproduction number of the latent cell model (2) is *strictly less* than that of the standard three-component model (1). Therefore, the stability of the the uninfected state is enhanced by the inclusion of the latently-infected cell population. Namely, there are more values of $\lambda, d_T, d_I, d_V, k$ and N which correspond to $R_L \leq 1$ than $R_0 \leq 1$. From a modeling standpoint, this result is somewhat intuitive. Because (2) assumes that a fraction of newly infected cells become latently infected and the latter can only activate (becoming actively productive) or die, the average number of infected cells generated by the introduction of a single infected cell into a susceptible system is decreased in comparison to a model without latently infected cells, namely (1). Hence, one should expect that the basic reproduction number, representing this average number of infected cells, does in fact decrease. Another consequence of this result is that there exist a number of parameter values for which $R_0 > 1$ but $R_L \leq 1$, and in such cases the solutions of (1) tend to E_{NI} while those of (2) tend to E_I as $t \to \infty$. Clearly, the converse ($R_0 \leq 1$ but $R_L > 1$) is not possible by the above inequality. In fact, we may rewrite the ratio of reproductive numbers as

$$Q = 1 - \frac{pd_L}{d_L + \alpha}$$

so that the difference between R_0 and R_L is greatest for large values of p and d_L, but small values of α. With the representative parameter values given in Table 1, we see that

$$R_L \approx 5.978 \quad \text{and} \quad R_0 \approx 6.154.$$

Hence, the change in system behavior caused by the difference between the reproduction numbers appears somewhat negligible, as both values are significantly larger than their respective bifurcation points. Additionally, $Q = 0.97$ in this case, so that the relative difference between R_0 and R_L is merely

$$\frac{R_0 - R_L}{R_0} = 1 - Q = 3\,\%.$$

Exactly quantifying this relative change, however, is difficult since many of the parameter values of Table 1, in particular k, p, α, and d_L, are not well-established, and hence this percentage could be much larger or perhaps even smaller. For example, if we utilize the smallest value of $\alpha = 3 \times 10^{-3}$, stemming from [24], and the largest values of $p = 0.1$ [36] and $d_L = 0.24$ [24], then a simple computation shows that $Q = 0.9$. Hence, the relative difference between reproductive ratios could possibly be as large as 10 %, though more conservative estimates of the associated parameters place this value between 1 % and 5 %.

Regardless of the quantified distinction between the reproductive ratios, it seems somewhat counterintuitive that $R_L < R_0$, especially since so many authors [1,2,6,7,9,10,18,19,23,29,33] have detailed the large degree to which latent reservoirs contribute to the increased persistence of HIV infection via viral rebound after treatment with ART. Hence, the result of the mathematical analysis, namely that the effects of latent infection *reduce* the basic reproductive ratio, seems to contradict this theory. However, as we previously stated, the alterations in the mathematical model explain this effect. Additionally, the reproductive ratio is but one parameter, and so it seems unlikely that this particular metric will completely determine the realistic behavior of the system. In fact, a more detailed analysis of the behavior of solutions over the timescales of biological relevance, rather than considering only the limiting behavior as $t \to \infty$, will demonstrate the shortcomings of the basic reproductive ratio. We illustrate this using the effects of antiretroviral therapy and some associated computational results within the next section.

Antiretroviral Therapy

In order to further contrast these two models and the effects of the latent cell population, we will introduce additional parameters to represent the application of antiretroviral therapy. The inclusion of ART will allow us to determine the range of drug efficacies that distinguish between the limiting dynamics of (1) and (2) and further elucidate the differing behaviors of the two models.

Two classes of antiretroviral drugs are often used to reduce the viral load and limit the infected T-cell population. One class is known as Reverse Transcriptase Inhibitors (RTIs), which prevent the reverse transcription of viral RNA to DNA. The other category is Protease Inhibitors (PIs), which prevent HIV-1 protease from cleaving the HIV polyprotein into functional units, thereby causing infected cells to produce immature virus particles that are not capable of infecting additional cells. In this way, RTIs serve to reduce the rate of infection of activated CD4+ T-cells within the model, whereas PIs decrease the number of new infectious virions that are produced. Both drugs thus diminish the propagation of the virus [17,31]. While we expect that latently infected cells may absorb PIs and that such cells, when

activated, will produce noninfectious virus, we will instead assume that PIs have no effect on the proportion of cells that are latently infected. This is in line with some experimental findings, that suggest that antiretroviral drugs do not effectively block replication of virus from the latent reservoir [8]. Hence, in our model, susceptible T-cells may be inhibited with either RTIs, or PIs, or they may become infected. Infected cells may be inhibited with PIs, and cells inhibited with one drug may be inhibited with the other. In the presence of these two inhibitors, the model equations (2) are modified to become:

$$\begin{cases} \dfrac{dT}{dt} = \lambda - d_T T - k(1-\epsilon_{RT})TV_I, \\ \dfrac{dI}{dt} = (1-p)k(1-\epsilon_{RT})TV_I + \alpha L - d_I I, \\ \dfrac{dL}{dt} = pk(1-\epsilon_{RT})TV_I - \alpha L - d_L I, \\ \dfrac{dV_I}{dt} = N(1-\epsilon_{PI})d_I I - d_V V_I. \end{cases} \tag{5}$$

where $\epsilon_{RT}, \epsilon_{PI} \in [0, 1]$ are the efficacies of RTIs and PIs, and V_I represents the population of infectious virions. We may include the number of non-infectious virions V_{NI}, with the total viral load $V = V_I + V_{NI}$, but V_{NI} decouples from the remaining equations, and hence plays no role in the evolution of the system.

To compute the steady states and basic reproduction number for (5), we may reproduce the analysis of (2), but clearly the new terms are introduced only where the parameters k and N appear. Thus, we need only replace k with $k(1-\epsilon_{RT})$ and N with $N(1-\epsilon_{PI})$. The new basic reproduction number then becomes

$$R_L^\epsilon = \frac{kN(1-\epsilon)\lambda}{d_T d_V} \cdot \frac{(1-p)d_L + \alpha}{d_L + \alpha}, \tag{6}$$

where we define the quantity $\epsilon = \epsilon_{RT} + \epsilon_{PI} - \epsilon_{RT}\epsilon_{PI}$, so that

$$1 - \epsilon = (1-\epsilon_{RT})(1-\epsilon_{PI}).$$

Since (5) is identical to (2) with the minor change in parameter values described above, Theorems 2 and 3 hold for (5) with the corresponding value R_L^ϵ instead of R_L.

Writing the corresponding viral steady state for (5) we find

$$\overline{V} = \frac{d_T R_L}{k}(1-\epsilon_{PI}) - \frac{d_T}{k(1-\epsilon_{RT})}$$

and we notice that its partial derivative

$$\frac{\partial \overline{V}}{\partial \epsilon_{RT}} = -\frac{d_T}{k(1-\epsilon_{RT})^2}$$

is large, especially when $\epsilon_{RT} \approx 1$. Thus, $\overline{V}$ is sensitive to small changes in ϵ_{RT} at large efficacies, and this sensitivity increases with the efficacy of the RTI. Hence, this model does not realistically describe the persistence of low-level viremia in patients on reverse transcriptase inhibitors, as previously addressed within [29]. However, we note that

$$\frac{\partial \overline{V}}{\partial \epsilon_{PI}} = -\frac{d_T R_L}{k},$$

which is constant for all values of ϵ_{PI}, and does not possess the same sensitivity. Thus, to simplify the analysis, we will assume throughout that only PIs are used, and hence $\epsilon = \epsilon_{PI}$ while $\epsilon_{RT} = 0$. We note, however, that the analysis with RT inhibitors could be performed in a similar manner.

Upon incorporating the use of antiretroviral drugs into (1), the system becomes

$$\begin{cases} \dfrac{dT}{dt} = \lambda - d_T T - k(1-\epsilon_{RT})TV_I, \\ \dfrac{dI}{dt} = k(1-\epsilon_{RT})TV_I - d_I I, \\ \dfrac{dV_I}{dt} = N(1-\epsilon_{PI})d_I I - d_V V_I. \end{cases} \tag{7}$$

with associated basic reproduction number

$$R_0^\epsilon = \frac{kN(1-\epsilon)\lambda}{d_T d_V}. \tag{8}$$

As for (5), the stability results for (1) contained in an earlier section hold for (7) by replacing R_0 with R_0^ϵ. Comparing the two values R_0^ϵ and R_L^ϵ, we see that their ratio is again Q given by (4), so that $R_L^\epsilon = QR_0^\epsilon$. As before, since $Q < 1$ we find $R_L^\epsilon < R_0^\epsilon$ and even with the incorporation of ART, the latent cell population *decreases* the basic reproduction number of the system. With the representative parameter values given in Table 1, we see that the basic reproduction numbers associated with (5) and (7) are

$$R_L^\epsilon \approx 2.027(1-\epsilon) \quad \text{and} \quad R_0^\epsilon \approx 2.087(1-\epsilon).$$

Hence, the critical drug efficacy (i.e, the efficacy needed in order for the uninfected state to be realized) for (7) is $\epsilon_0^{crit} = 0.521$, which only differs mildly from the value of the critical drug efficacy for (5), namely $\epsilon_L^{crit} = 0.506$. Thus, the antiretroviral therapy must attain an efficacy only 3 % greater in order to achieve the analogous effect. From this analysis, it would seem that the establishment of a latent reservoir should not strengthen a continued infection since the drug efficacy necessary to drive the system to an uninfected equilibrium is actually less for (5) than for (7). This result seems to greatly contradict the known issues that scientists have faced regarding the eradication of the viral reservoir. However, the resolution of these seemingly opposing viewpoints is made quite clear by precise numerical simulations.

As an illustrative example of the difference in long-time dynamics between the two models, we may choose values of ϵ which yield $R_0^\epsilon > 1$ and $R_L^\epsilon < 1$ and measure their corresponding behavior. A representative simulation is presented in Fig. 3. To differentiate between the corresponding viral loads, we will denote the infectious virus population associated with (7) by $V_{3CM}(t)$ and its latent model analogue by $V_{Latent}(t)$ as in the figure. In this case, we choose $\epsilon = 0.519$ and find $R_0^\epsilon = 1.003$ and $R_L^\epsilon = 0.974$. Hence, from the known results of the section concerning three-component model and Theorem 3, we may deduce that $V_{3CM}(t) \to \frac{d_T}{k}(R_0^\epsilon - 1) \approx 2 \times 10^3$ as $t \to \infty$, while $V_{Latent}(t) \to 0$ as $t \to \infty$. However, one can distinctly see from Fig. 3 that the early decay rate of V_{3CM} is much greater than that of V_{Latent}.

Notice that the effects of latent infection do not influence the viral load for the first thirty days of treatment as $V_{3CM}(t)$ and $V_{Latent}(t)$ follow the same approximate trajectory during this time period. However, once the latently infected T-cell population grows sufficiently large, the effects are tremendous. Throughout the first 3 years of continuous treatment, V_{3CM} diminishes greatly, past 10^{-10} in fact, while V_{Latent} remains $O(1)$ even up to day 1,000. Certainly this

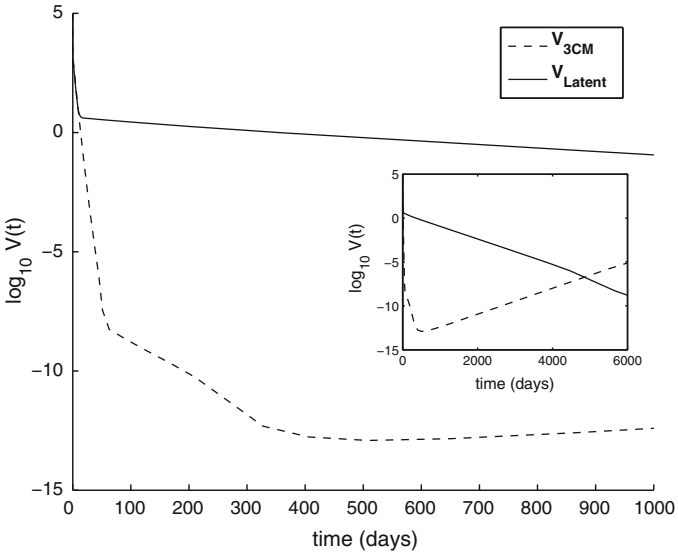

Fig. 3 Viral loads for (5) and (7) with parameter values given in Table 1 and $\epsilon = 0.519$. This value of ϵ yields $R_0^\epsilon = 1.003$ and $R_L^\epsilon = 0.974$, respectively. The *inset figure* includes the viral behavior for $t \in [0, 6000]$ days

seems strange as $R_0^\epsilon > 1$ implies a persistent virus population must develop for (7) and $R_L < 1$ dictates the eventual elimination of the viral population for the latent model. Within the inset figure, it can be seen that the behavior predicted by the basic reproduction numbers does eventually occur, that is, values of V_{3CM} rebound and tend to a positive equilibrium, while those of V_{Latent} continue their slow, steady decline to eradication. Unfortunately, these events occur nearly 15 years after the introduction of ART and well outside the timescale of biological relevance. Hence, it appears that the values of R_0^ϵ and R_L^ϵ alone cannot provide sufficient information to account for the realistic biological dynamics of the model due to the change in timescales and decay rates introduced by the latent cell population. A better estimate of the behavior would certainly be given by the rates of decay to eradication, but precise estimates on these quantities are more difficult to obtain analytically. Instead, we examine a slightly different metric of viral persistence or clearance.

The feature of viral clearance that one must capture here is not just the decay of the viral load, but a sufficiently rapid speed of decay so as to be realized within a time period of biological relevance. Hence, we consider a specific value of the virus population to represent clearance, and proceed to study the minimum arrival time of the viral load to that value. In this vein, we define the functions

$$P_n(r) = \inf\left\{t > 0 : \log_{10}\left(V_{3CM}(t)\right) \leq -n \text{ for } R_0^\epsilon = r\right\}$$

and

$$Q_n(r) = \inf\left\{t > 0 : \log_{10}\left(V_{Latent}(t)\right) \leq -n \text{ for } R_L^\epsilon = r\right\}.$$

We note that either of these functions may become infinite if the population of virions fails to reach the prescribed value for any positive time. For example, $P_5(2) = Q_5(2) = \infty$, since neither viral load obtains a value as small as 10^{-5} for a corresponding reproductive ratio of

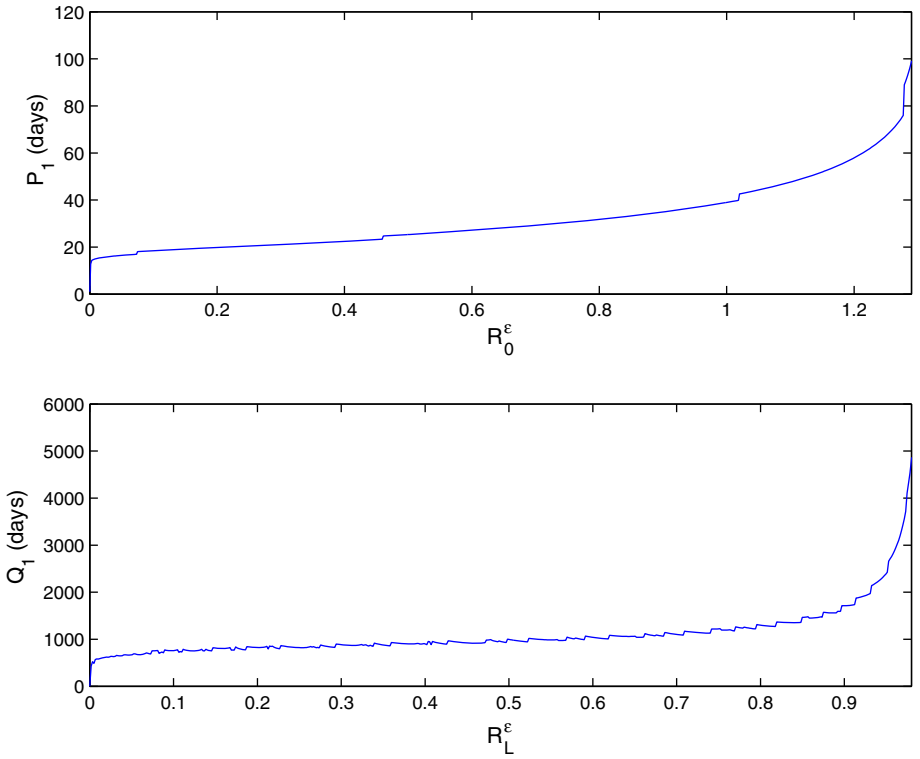

Fig. 4 Comparison of $P_5(R_0^\epsilon)$ and $Q_5(R_L^\epsilon)$

2, while $P_5(0.6) \approx 25$ and $Q_5(0.6) \approx 1,000$ as represented in Fig. 4. Unlike the stability of equilibria, the values of $P_n(r)$ and $Q_n(r)$ will depend upon the initial population values that are chosen. Within the present study, however, we will continue to utilize the initial populations of previous sections to serve as a representative example.

We first select the value of 10^{-5} copies per ml for our definition of viral eradication and study the associated times to eradication provided by the functions P_5 and Q_5. Namely, what we are assuming is that once the viral population is suitably dilute—in this case less that 10^{-5} copies per ml—then the infection has been cleared and no rebound can occur. Figure 4 provides a comparison of P_5 and Q_5 for differing values of R_0^ϵ and R_L^ϵ, respectively. Though their general shapes are quite similar, the associated time periods differ dramatically. Typical values of P_5 range from 20 to 100 days, while the majority of values of Q_5 range between 1,000 and 3,000 days. As can be seen in Fig. 4, even if the efficacy of the RT inhibitor, ϵ, approaches 100 %, and thus R_0^ϵ approaches zero, V_{3CM} requires around 15 days to reach a value of 10^{-5}. In this same situation, R_L^ϵ approaches zero, but V_{Latent} requires nearly 500–1,000 days to reach a value of 10^{-5}. Thus, even for values of R_L^ϵ which are significantly less than one, we see that it would require nearly 3 years for the viral load to reach this threshold due to the influence of latent infection. In addition, we see that V_{3CM} will reach values of 10^{-5} even if $R_0^\epsilon > 1$, and this will occur within 100 days, almost ten times faster than it would take V_{Latent} to reach the same value for a constant drug efficacy around 90 %.

Considering that the biological detection threshold for commercially-available assays is around 50 viral copies per ml [4,12], one possibility is that the 10^{-5} threshold above has been

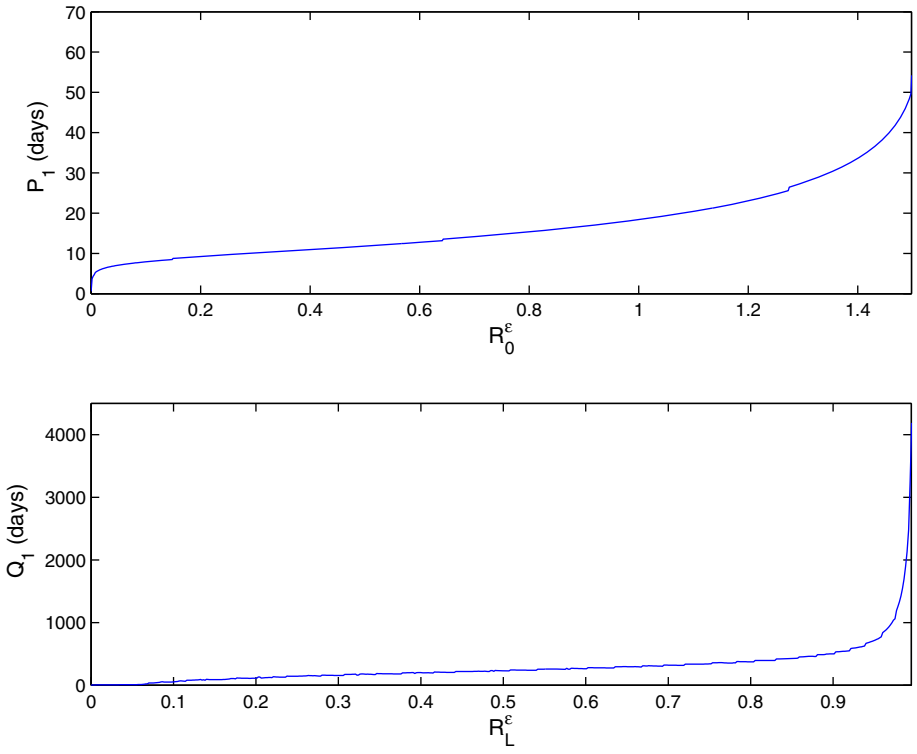

Fig. 5 Comparison of $P_1(R_0^\epsilon)$ and $Q_1(R_L^\epsilon)$

chosen too small in Fig. 4 to effectively serve as a realistic measure of eradication. Hence, we consider P_1 and Q_1 and perform a similar analysis. Figure 5 contains these simulations and displays a decrease in the time necessary to reach the defined threshold of 10^{-1}. However, even for a 70 % constant drug efficacy, in which case $R_L^\epsilon = 0.6$, we see that approximately 1 year of continuous ART would still be required to reach a viral load of 0.1 copies per ml for (5). Additionally, values of P_1 remain around 60 for (7) even if R_0^ϵ is near 1.5, which exceeds the bifurcation point by nearly 50 %. Thus, if we define viral clearance as a decay in the viral load to 0.1 copies per ml within six months of treatment, then (7) would require R_0^ϵ to be less than 1.5 while (5) would require R_L^ϵ to be less than 0.2. Obviously, a much wider range of parameter values will yield $R_0^\epsilon < 1.5$ than $R_L^\epsilon < 0.2$, and we see that the latent T-cell population does, in fact, extend the period of time during which viremia persists, even though the behavior as $t \to \infty$, as given by Theorems 2 and 3, may provide seemingly contrary information.

From this, the biological influence of latent infection becomes clear - the time needed to decrease the viral load to values from which rebound is unlikely or unable to occur is increased by a factor of ten or twenty. Hence, the value of the basic reproduction number alone does not represent a proper definition for viral persistence or eradication, and the functions provided above $P_n(r)$ and $Q_n(r)$, for well-chosen values of n, possess the information required to better determine the behavior of the infection. Further analysis can be performed for smaller (and negative) values of n, but the results discussed above are typical. In the next section, we prove Theorems 1, 2, and 3 regarding the qualitative behavior of the latent infection model.

Proofs of Main Theorems

With the analysis concluded, we finally prove the main results of the previous sections. In what follows, C will be used to denote a positive, but arbitrary constant which may change from line to line. First, we prove the existence, uniqueness, and positivity of solutions.

Proof (*Theorem* 1) While one may prove that a certain positive set remains invariant under the flow (as in [13]), this requires assumptions which bound the initial data from above. In our proof, we utilize a continuity argument instead and do not assume any upper bounds on initial data. Using the Picard–Lindeloff theorem and the quadratic nature of the equation, the local-in-time existence of a unique, C^1 solution follows immediately. Hence, we will concentrate on proving positivity of solutions as long as they remain continuous, and this property will yield bounds on the growth of solutions. From the bounds obtained below, then, it follows that the solution exists globally and is both unique and continuously differentiable for all $t > 0$. Define

$$T^* = \sup\{t \geq 0 : T(s), I(s), L(s), V(s) > 0, \text{ for all } s \in [0, t]\}.$$

Since each initial condition is nonnegative and the solution is continuous, there must be an interval on which the solution remains positive, and we see that $T^* > 0$. Then on the interval $[0, T^*]$ we estimate each term.

Lower bounds on I, L, and V instantly follow since the decay terms are linear. More specifically, we find

$$\frac{dI}{dt} = (1-p)kTV + \alpha L - d_I I \geq -d_I I$$

and thus

$$I(t) \geq I(0)e^{-d_I t} > 0$$

for all $t \in [0, T^*]$. Similarly, for the latent T-cell population

$$\frac{dL}{dt} = pkTV - (d_L + \alpha)L \geq -(d_L + \alpha)L$$

and thus

$$L(t) \geq L(0)e^{-(d_L+\alpha)t} > 0$$

for all $t \in [0, T^*]$. The positivity of the virion population follows in the same manner since

$$\frac{dV}{dt} = Nd_I I - d_V V \geq -d_V V$$

and thus

$$V(t) \geq L(0)e^{-d_V t} > 0$$

for all $t \in [0, T^*]$. The positivity of T requires extra effort since it decreases due to the nonlinearity. We first construct an upper bound on $\frac{dT}{dt}$ as

$$\frac{dT}{dt} = \lambda - \mu T - kTV \leq \lambda$$

and thus

$$T(t) \leq T(0) + \lambda t \leq C(1+t).$$

Next, we sum the equations for I, L, and V, and by positivity of these functions, obtain upper bounds on each one. Using the upper bound on $T(t)$, we find

$$\frac{d}{dt}(I+L+V) = kTV + (N-1)d_I I - d_L L - d_V V \leq C(1+t)(I+L+V).$$

By Gronwall's Inequality, we have

$$I(t) + L(t) + V(t) \leq Ce^{Ct^2}$$

for $t \in [0, T^*]$. Since $I(t)$ and $L(t)$ are positive on this interval, the same upper bound follows on $V(t)$ alone. With this, we can now obtain a lower bound on T. We find

$$\frac{dT}{dt} = \lambda - d_T T - kTV \geq -d_T T - kTV \geq -C(1+e^{Ct^2})T$$

or stated equivalently

$$\frac{dT}{dt} + C(1+e^{Ct^2})T \geq 0.$$

It follows that

$$\frac{d}{dt}\left(T(t)e^{C\int_0^t (1+e^{C\tau^2})d\tau}\right) \geq 0$$

and

$$T(t) \geq T(0)e^{-C\int_0^t (1+e^{C\tau^2})d\tau} > 0$$

for $t \in [0, T^*]$. Finally, if $T^* < \infty$, then all functions are strictly positive at time T^*, contradicting its definition as the supremum of such values. Hence, we find $T^* = \infty$ and the result follows. □

Next, we sketch the proof of the local stability results.

Proof (*Theorem* 2) As is somewhat standard, we proceed by linearizing the system and using the Routh–Hurwitz criterion to determine conditions under which the linear system possesses only negative eigenvalues. Then, as a consequence of the Hartman–Grobman Theorem, the local behavior of the linearized system is equivalent to that of the nonlinear system.

First, we compute the Jacobian evaluated at the uninfected equilibrium $E_{NI} = \left(\frac{\lambda}{d_T}, 0, 0, 0\right)$, resulting in

$$J(E_{NI}) = \begin{bmatrix} -d_T & 0 & 0 & -\frac{k\lambda}{d_T} \\ 0 & -d_I & \alpha & \frac{k(1-p)\lambda}{d_T} \\ 0 & 0 & -d_L - \alpha & \frac{kp\lambda}{d_T} \\ 0 & Nd_I & 0 & -d_V \end{bmatrix}.$$

From this, we compute the associated characteristic polynomial for eigenvalues η

$$\eta^3 + A_1\eta^2 + A_2\eta + A_3 = 0, \tag{9}$$

where

$$A_1 = d_V + d_I + d_L + \alpha,$$
$$A_2 = d_I d_V + (d_L + \alpha)(d_I + d_V) - \frac{(1-p)\lambda N k d_I}{d_T},$$
$$A_3 = (d_L + \alpha) d_I d_V - \frac{\lambda N k d_I}{d_T}((1-p)d_L + \alpha).$$

The Routh–Hurwitz criterion requires $A_1, A_2, A_3 > 0$ and $A_1 A_2 - A_3 > 0$. Using the inequality

$$\frac{(1-p)(d_L+\alpha)}{(1-p)d_L + \alpha} = 1 - \frac{p\alpha}{(1-p)d_L + \alpha} < 1, \tag{10}$$

and the previous condition $R_L < 1$, we find $A_1, A_2, A_3 > 0$. Finally, using (10), we see that $A_2 > d_I d_V (1 - R_L)$, and clearly $A_1 > d_L + \alpha$. Therefore, we find

$$A_1 A_2 > d_I d_V (d_L + \alpha)(1 - R_L) = A_3$$

and the Routh–Hurwitz criteria are satisfied. Thus, $R_L < 1$ implies that all eigenvalues of the linearized system are negative, and hence the local asymptotic stability of E_{NI} follows. Conversely, if $R_L > 1$, then the linearized system possesses at least one positive eigenvalue, and the equilibrium is unstable.

The analysis for E_I is similar to that of E_{NI} and we omit it for brevity. Finally, the local behavior of the system for $R_L = 1$ is implied by the result of Theorem 3. □

Lastly, we include a proof of the previously stated global stability theorem.

Proof (*Theorem* 3) As in [20] for the case of (1), we will prove the global stability using a Lyapunov function [25]. We will denote the uninfected equilibrium by $(T^0, 0, 0, 0)$. First, note that the quantity

$$T(t) - T^0 - T^0 \ln\left(\frac{T(t)}{T^0}\right)$$

vanishes when evaluated at $T(t) = T^0$ and is nonnegative as long as $T(t) > 0$ by a simple application of Taylor's Theorem. Next, define

$$U(t) = ((1-p)d_L + \alpha)\left[T(t) - T^0 - T^0 \ln\left(\frac{T(t)}{T^0}\right)\right] + (d_L + \alpha)\left[I(t) + \frac{1}{N}V(t)\right] + \alpha L(t).$$

Notice that U is C^1, nonnegative, and tends to infinity as T, I, L, and V do. Additionally, U is identically zero if and only if it is evaluated at the uninfected equilibrium point. We compute the derivative along trajectories and find

$$\frac{dU}{dt} = ((1-p)d_L + \alpha)\left(1 - \frac{T^0}{T}\right)[\lambda - d_T T - kTV] + (d_L + \alpha)\left[(1-p)kTV + \alpha L - d_I I + \frac{1}{N}(N d_I I - d_V V)\right] + \alpha[pkTV - (\alpha + d_L)L]$$

The I, L, and TV terms all cancel and after using the definition of T^0, we are left with

$$\begin{aligned}\frac{dU}{dt} &= ((1-p)d_L+\alpha)(\lambda - d_T T)\left(1-\frac{\lambda}{d_T T}\right)\\ &\quad + \left[((1-p)d_L+\alpha)kT^* - (d_L+\alpha)\frac{d_V}{N}\right]V\\ &= -\frac{(1-p)d_L+\alpha}{d_T T}(\lambda - d_T T)^2 + \frac{(d_L+\alpha)d_V}{N}(R_L-1)V.\end{aligned}$$

Thus, under the assumption that $R_L \le 1$, we see that $\frac{dU}{dt} \le 0$ for all positive values of T, I, L, and V, and the global asymptotic stability follows by LaSalle's Invariance Principle [35].

Turning to the infected equilibrium, none of the end values are zero, so we denote this steady state by (T^*, I^*, L^*, V^*) and define

$$\begin{aligned}U(t) &= ((1-p)d_L+\alpha)\left[T(t) - T^* - T^*\ln\left(\frac{T(t)}{T^*}\right)\right]\\ &\quad + (d_L+\alpha)\left[I(t) - I^* - I^*\ln\left(\frac{I(t)}{I^*}\right) + \frac{1}{N}\left(V(t) - V^* - V^*\ln\left(\frac{V(t)}{V^*}\right)\right)\right]\\ &\quad + \alpha\left[L(t) - L^* - L^*\ln\left(\frac{L(t)}{L^*}\right)\right].\end{aligned}$$

As before, this function is nonnegative and identically zero only when evaluated at the infected equilibrium. Computing the derivative along trajectories yields

$$\begin{aligned}\frac{dU}{dt} &= ((1-p)d_L+\alpha)\left(1-\frac{T^*}{T}\right)[\lambda - d_T T - kTV]\\ &\quad + (d_L+\alpha)\left[\left(1-\frac{I^*}{I}\right)((1-p)kTV + \alpha L - d_I I)\right.\\ &\quad \left. + \frac{1}{N}\left(1-\frac{V^*}{V}\right)(Nd_I I - d_V V)\right] + \alpha\left(1-\frac{L^*}{L}\right)[pkTV - (\alpha+d_L)L]\\ &= ((1-p)d_L+\alpha)[\lambda - d_T T - kTV]\\ &\quad + (d_L+\alpha)\left[(1-p)kTV + \alpha L - d_I I + \left(d_I I - \frac{d_V}{N}V\right)\right]\\ &\quad + \alpha[pkTV - (\alpha+d_L)L] - ((1-p)d_L+\alpha)\left[\frac{\lambda T^*}{T} - d_T T^* - kT^*V\right]\\ &\quad -(d_L+\alpha)\left[\frac{(1-p)kTVI^*}{I} + \frac{\alpha L I^*}{I} - d_I I^* + \frac{d_I I V^*}{V} - \frac{d_V V^*}{N}\right]\\ &\quad + \alpha\left[\frac{pkTVL^*}{L} - (\alpha+d_L)L^*\right].\end{aligned}$$

Nicely, the I, L, V, and TV terms all vanish and what remains is

$$\begin{aligned}\frac{dU}{dt} &= ((1-p)d_L+\alpha)\left[\lambda - d_T T + d_T T^* - \frac{\lambda T^*}{T}\right]\\ &\quad + (d_L+\alpha)\left[-(1-p)k\frac{TVI^*}{I} - \alpha\frac{LI^*}{I} + d_I I^* - d_I\frac{IV^*}{V} + d_V\frac{V^*}{N}\right.\end{aligned}$$

$$+\alpha L^* - \frac{\alpha pk}{d_L+\alpha}\frac{TVL^*}{L}\Bigg]$$
$$=: I + II.$$

For I, we factor out a $d_T T^*$ term and use the form of T^* to find

$$\begin{aligned} I &= (d_L+\alpha)d_T T^*\left[R_L + 1 - \frac{T}{T^*} - R_L\frac{T^*}{T}\right] \\ &= (d_L+\alpha)d_T T^*\left[2 - \frac{T}{T^*} - \frac{T^*}{T} + (R_L-1)\left(1-\frac{T^*}{T}\right)\right] \\ &= (d_L+\alpha)d_T T^*\left[2 - \frac{T}{T^*} - \frac{T^*}{T}\right] + (d_L+\alpha)d_T T^*(R_L-1)\left(1-\frac{T^*}{T}\right). \end{aligned}$$

For II, we factor an L^* term and use the identities

$$T^*V^* = \frac{d_L+\alpha}{kp}L^* \quad \text{and} \quad Nd_I I^* = d_V V^*$$

to find

$$\begin{aligned} II &= (d_L+\alpha)L^*\Bigg[\alpha + \frac{d_I I^*}{L^*} + \frac{d_V V^*}{NL^*} - (1-p)k\frac{TVI^*}{L^*I} - \frac{d_I I^*}{L^*}\frac{IV^*}{I^*V} \\ &\quad - \frac{\alpha pk}{d_L+\alpha}\frac{TV}{L} - \alpha\frac{LI^*}{L^*I}\Bigg], \\ &= (d_L+\alpha)L^*\Bigg[\alpha + \frac{2((1-p)d_L+\alpha)}{p} - \frac{(1-p)(d_L+\alpha)}{p}\frac{TVI^*}{T^*V^*I} \\ &\quad - \frac{(1-p)d_L+\alpha}{p}\frac{IV^*}{I^*V} - \alpha\frac{TVL^*}{T^*V^*L} - \alpha\frac{LI^*}{L^*I}\Bigg], \\ &= \frac{(d_L+\alpha)L^*}{p}\Bigg[((1-p)d_L+\alpha)\left(2-\frac{IV^*}{I^*V}\right) - (1-p)(d_L+\alpha)\frac{TVI^*}{T^*V^*I} \\ &\quad + \alpha p\left(1 - \frac{TVL^*}{T^*V^*L} - \frac{LI^*}{L^*I}\right)\Bigg]. \end{aligned}$$

Thus, combining the rearrangements of I and II, we find

$$\begin{aligned} \frac{dU}{dt} &= (d_L+\alpha)d_T T^*\left[2 - \frac{T}{T^*} - \frac{T^*}{T}\right] + (d_L+\alpha)d_T T^*(R_L-1)\left(1-\frac{T^*}{T}\right) \\ &\quad + \frac{(d_L+\alpha)L^*}{p}\Bigg[((1-p)d_L+\alpha)\left(2-\frac{IV^*}{I^*V}\right) - (1-p)(d_L+\alpha)\frac{TVI^*}{T^*V^*I} \\ &\quad + \alpha p\left(1 - \frac{TVL^*}{T^*V^*L} - \frac{LI^*}{L^*I}\right)\Bigg]. \end{aligned}$$

The second term simplifies to combine with those in the third term since

$$(d_L+\alpha)d_T T^*(R_L-1) = \frac{(d_L+\alpha)L^*((1-p)d_L+\alpha)}{p}$$

and therefore the expression becomes

$$\frac{dU}{dt} = (d_L+\alpha)d_T T^*\left[2-\frac{T}{T^*}-\frac{T^*}{T}\right] + \frac{(d_L+\alpha)L^*}{p}\left[((1-p)d_L+\alpha)\left(3-\frac{T^*}{T}-\frac{IV^*}{I^*V}\right)-(1-p)(d_L+\alpha)\frac{TVI^*}{T^*V^*I} + \alpha p\left(1-\frac{TVL^*}{T^*V^*L}-\frac{LI^*}{L^*I}\right)\right].$$

Since $(1-p)(d_L+\alpha) = (1-p)d_L+\alpha-\alpha p$, we add and subtract αp within the first term of the second line and place the extra components in the terms on the third line to arrive at

$$\frac{dU}{dt} = (d_L+\alpha)d_T T^*\left[2-\frac{T}{T^*}-\frac{T^*}{T}\right] + \frac{(d_L+\alpha)L^*}{p}\left[(1-p)(d_L+\alpha)\left(3-\frac{T^*}{T}-\frac{TVI^*}{T^*V^*I}-\frac{IV^*}{I^*V}\right) + \alpha p\left(4-\frac{T^*}{T}-\frac{TVL^*}{T^*V^*L}-\frac{LI^*}{L^*I}-\frac{IV^*}{I^*V}\right)\right].$$

Finally, each of the resulting terms above are nonpositive because the arithmetic mean is greater than the geometric mean, or more specifically,

$$\frac{1}{2}\left(\frac{T}{T^*}+\frac{T^*}{T}\right) \geq \sqrt{\frac{T}{T^*}\cdot\frac{T^*}{T}} = 1,$$

$$\frac{1}{3}\left(\frac{T^*}{T}+\frac{TVI^*}{T^*V^*I}+\frac{IV^*}{I^*V}\right) \geq \sqrt[3]{\frac{T^*}{T}\cdot\frac{TVI^*}{T^*V^*I}\cdot\frac{IV^*}{I^*V}} = 1,$$

$$\frac{1}{4}\left(\frac{T^*}{T}+\frac{TVL^*}{T^*V^*L}+\frac{LI^*}{L^*I}+\frac{IV^*}{I^*V}\right) \geq \sqrt[4]{\frac{T^*}{T}\cdot\frac{TVL^*}{T^*V^*L}\cdot\frac{LI^*}{L^*I}\cdot\frac{IV^*}{I^*V}} = 1.$$

Hence, $\frac{dU}{dt} \leq 0$ for all positive values of T, I, L, and V. As in the uninfected case, the conclusion then follows directly from LaSalle's Invariance Principle. □

Discussion

In order to realistically describe and predict the effects of latent HIV infection, models of HIV-1 dynamics and the associated mathematical tools must be capable of explaining the rich set of dynamics inherent within their formulation. We have explored the steady states and asymptotic behavior of the basic three-component model and its well-known variant which includes the effects of latent infection. A rigorous analysis of the large time behavior of these systems displays a reduction in the basic reproduction number due to the appearance of the latently infected T-cell population, and at first glance seems contradictory to the known difficulties of eradicating the latent reservoir with antiretroviral therapy. After undertaking a more detailed analysis here, we find that even though the inclusion of latent T-cells allows for a wider range of parameter values to induce viral eradication as $t \to \infty$, the rate at which this decay occurs under ART is retarded so significantly that, in the majority of cases, the decay could only occur outside time periods of biological relevance. This analysis highlights two major points. First and foremost, the latent cell population drastically extends the lifespan of infection. This can be seen from the rates of decay displayed within the previous section by the functions P and

Q. However, since this property cannot be detected at the level of the basic reproduction number, a second major point becomes clear. The standard tools of computing equilibrium states and the differing conditions under which a system may tend to these states as $t \to \infty$ is clearly insufficient to describe, or more importantly predict, the realistic dynamics that these equations model. Hence, a more refined analysis which investigates not only the end states, but the rate of propagation to a supposed equilibrium value within a specified time period, is clearly needed to describe the propagation of HIV, at least when considering the effects of latent infection.

Of course, our study is not all-inclusive. In attempting to address the question of latently infected cell reservoirs, we have ignored other potential reservoirs of HIV, such as those occurring within the brain, testicles, and dendritic cells [6]. The extent of viral replication in compartments other than resting CD4 + T-cells in patients receiving antiretroviral therapy for extended periods of time has yet to be fully delineated. One may also adapt the model to account for other viral reservoirs and incorporate the immune system response to a viral load. In addition, we assumed the use of antiretroviral therapy that included only PIs. Certainly, the effects of RTIs could also be included, though the picture becomes slightly more complex, and the results are similar. One can also study effects arising from a number of additional aspects including

1. A secondary infective population, such as macrophages [13]
2. Pharmacological delays due to drug activation
3. The residual effects of decaying drug efficacy or periodic ART schedules
4. Spatial effects, such as those characterized by diffusion models and multiple compartment models
5. Uncertainty arising from the measurement of parameter values or fluctuations across populations of individuals in the form of random coefficients or stochastic differential equations
6. Successive mutation of HIV virions

That being said, the effects of the latent cell population on viral behavior have been clearly documented within the current study, and it is greatly expected that even when additional mechanisms are incorporated within the model, the basic reproduction number will not serve as a descriptive parameter alone since it only describes the global asymptotic behavior of populations. Future work must examine the aforementioned issues within the context of latent infection using the exponential decay functions, P and Q, as a refinement of the mathematical analysis detailing the long time behavior of the model.

In conclusion, the dynamics of models that consider latent infection are so complex, even when spatial fluctuations are ignored, that a single parameter, in this case R_L or R_L^ϵ, cannot possibly dictate the realistic behavior of the corresponding populations. Instead, one must consider a number of factors including the time of validity inherent within the model, the average time periods underlying treatment, and the rates of decay associated with the trend to equilbrium.

Acknowledgments This work is supported by the National Science Foundation under awards DMS-0908413 and DMS-1211667. We also thank Prof. Mrinal Raghupathi (USNA) and ENS Peter Roemer (USN) for helpful comments.

References

1. Arlen, P.A., Brooks, D.G., Gao, L.Y., Vatakis, D., Brown, H.J., Zack, J.A.: Rapid expression of human immunodeficiency virus following activation of latently infected cells. J. Virol. **80**(3), 1599–1603 (2006)
2. Blankson, J.N., Persaud, D., Siliciano, R.F.: The challenge of viral reservoirs in HIV-1 infection. Annu. Rev. Med. **53**, 557–593 (2002)
3. Bonhoeffer, N., Con, J.M., Nowak, M.A.: Human immunodefciency virus drug therapy and virus load. J. Virol. **71**, 3275–3278 (1997)
4. Callaway, D.S., Perelson, A.S.: HIV-1 infection and low steady state viral loads. Bull. Math. Biol. **64**, 29–64 (2002)
5. Chen, H.Y., Di Mascio, M., Perelson, A., Gettie, A., Ho, D., et al: Determination of virus burst size in vivo using a single-cycle SIV in rhesus macaques, 9th conference on retroviruses and opportunistic infections (2002)
6. Chun, T.-W., Fauci, A.S.: Latent reservoirs of HIV: obstacles to the eradication of virus. Proc. Natl. Acad. Sci. **96**, 10958–10961 (1999)
7. Chun, T.W., Finzi, D., Margolick, J., et al.: In vivo fate of HIV-1-infected T cells: quantitative analysis of the transition to stable latency. Nat. Med. **1**, 1284–1290 (1995)
8. Chun, T.-W., Justement, J.S., Lempicki, R.A., Yang, J., Dennis, G., et al.: Gene expression and viral production in latently infected, resting CD4+ T-cells in viremic versus aviremic HIV-infected individuals. Proc. Natl. Acad. Sci. **100**(4), 1908–1913 (2003)
9. Chun, T.W., Carruth, L., Finzi, D., et al.: Quantification of latent tissue reservoirs and total body viral load in HIV-1 infection. Nature **387**, 183–188 (1997)
10. Chun, T.W., Stuyver, L., Mizell, S.B., et al.: Presence of an inducible HIV-1 latent reservoir during highly active antiretroviral therapy. Proc. Natl. Acad. Sci. **94**(24), 13193–13197 (1997)
11. De Boer, R.J., Ribeiro, R.M., Perelson, A.S.: Current estimates for HIV-1 production imply rapid viral clearance in lymphoid tissues. PLoS Comput. Biol. **6**(9), e1000906, 9 (2010). doi:10.1371/journal.pcbi.1000906. MR2741163 (2011j:92034)
12. Doyle, T., Smith, C., Vitiello, P., et al.: Plasma HIV-1 RNA detection below 50 copies/mL and risk of virologic rebound in patients receiving highly active antiretroviral therapy. Clin. Infect. Dis. **54**(5), 724–732 (2012). doi:10.1093/cid/cir936
13. Elaiw, A.M.: Global properties of a class of HIV models. Nonlinear Anal. Real World Appl. **11**(4), 2253–2263 (2010). doi:10.1016/j.nonrwa.2009.07.001. MR2661895 (2011m:92107)
14. Finzi, D., et al.: Latent infection of CD4+ T cells provides a mechanism for lifelong persistence of HIV-1, even in patients on effective combination therapy. Nat. Med. **5**, 512–517 (1999)
15. Haase, A.T., Henry, K., Zupancic, M., Sedgewick, G., Faust, R.A., et al.: Quantitative image analysis of HIV-1 infection in lymphoid tissue. Science **274**, 985–989 (1996)
16. Hockett, R.D., Kilby, J.M., Derdeyn, C.A., Saag, M.S., Sillers, M., et al.: Constant mean viral copy number per infected cell in tissues regardless of high, low, or undetectable plasma HIV RNA. J. Exp. Med. **189**, 1545–1554 (1999)
17. Janeway, C., Travers, P., Walport, M., Shlomchik, M.J.: Immunobiology 5: The Immune System in Health and Disease. Garland Publishing, New York (2001)
18. Kim, H., Perelson, A.S.: Viral and latent reservoir persistence in HIV-1-infect patients on therapy. PLoS Comput. Biol. **2**(10), e135 (2006). doi:10.1371/journal.pcbi.0020135
19. Kim, H., Perelson, A.S.: Dynamic characteristics of HIV-1 reservoirs. Curr. Opin. HIV AIDS **1**, 152–156 (2006)
20. Korobeinikov, A.: Global properties of basic virus dynamics models. Bull. Math. Biol. **66**(4), 879–883 (2004). doi:10.1016/j.bulm.2004.02.001. MR2255781 (2007e:34096)
21. Mohri, H., Bonhoeffer, S., Monard, S., Perelson, A., Ho, D.: Rapid turnover of T lymphocytes in SIV-infected rhesus macaques. Science **279**, 1223–1227 (1998)
22. Markowitz, M., Louie, M., Hurley, A., Sun, E., et al.: A novel antiviral intervention results in more accurate assessment of human immunodeficiency virus type 1 replication dynamics and T-cell decay in vivo. J. Virol. **777**, 5037–5038 (2003)
23. Perelson, A.S., Essunger, P., Cao, Y., Vesanen, M., Hurley, A., et al.: Decay characteristics of HIV-1-infected compartments during combination therapy. Nature **387**, 188–191 (1997)
24. Perelson, A.S., Kirschner, D.E., de Boer, R.: Dynamics of HIV infection of CD4+ T-cells. Math. Biosci. **114**, 81–125 (1993)
25. Perko, L.: Differential Equations and Dynamical Systems, Texts in Applied Mathematics, vol. 7, 3rd edn. Springer, New York (2001). doi:10.1007/978-1-4613-0003-8. MR1801796 (2001k:34001)
26. Pope, M., Haase, A.T.: Transmission, acute HIV-1 infection and the quest for strategies to prevent infection. Nat. Med. **9**, 847–852 (2003)

27. Ramratnam, B., Mittler, J.E., Zhang, L., Boden, D., Hurley, A., et al.: The decay of the latent reservoir of replication-competent HIV-1 is inversely correlated with the extent of residual viral replication during prolonged anti-retroviral therapy. Nat. Med. **6**, 82–85 (2000)
28. Ramratnam, B., Bonhoeffer, S., Binley, J., Hurley, A., Zhang, L., et al.: Rapid production and clearance of HIV-1 and hepatitis C virus assessed by large volume plasma apheresis. Lancet **354**, 1782–1785 (1999)
29. Rong, L., Perelson, A.S.: Modeling latently infected cell activation: viral and latent reservoir persistence, and viral blips in HIV-infected patients on potent therapy. PLoS Comput. Biol. **5**(10), e1000533, 18 (2009). doi:10.1371/journal.pcbi.1000533. MR2575020 (2011d:92047)
30. Rong, L., Perelson, A.S.: Modeling HIV persistence, the latent reservoir, and viral blips. J. Theor. Biol. **260**(2), 308–331 (2009). doi:10.1016/j.jtbi.2009.06.011. MR2973086
31. Rong, L., Feng, Z., Perelson, A.S.: Mathematical modeling of HIV-1 infection and drug therapy. Mathematical Modelling of Biosystems. Applied Optimization, vol. 102. Springer, Berlin (2008). MR2405002 (2009h:92037)
32. Sedaghat, A.R., Siliciano, J.D., Brennan, T.P., Wilke, C.O., Siliciano, R.F.: Limits on replenishment of the resting CD4+ T cell reservoir for HIV in patients on HAART. PLoS Pathog. **3**(8), e122 (2007)
33. Smith, R.J., Aggarwala, B.D.: Can the viral reservoir of latently infected CD4+ T cells be eradicated with antiretroviral HIV drugs? J. Math. Biol. **59**(5), 697–715 (2009). doi:10.1007/s00285-008-0245-4. MR2533762 (2010i:34121)
34. Stafford, M.A., Corey, L., Cao, Y., Daare, E.S., Ho, D.D., Perelson, A.S.: Modeling plasma virus concentration during primary HIV infection. J. Theor. Biol. **203**, 285–301 (2000)
35. Teschl, G.: Ordinary Differential Equations and Dynamical Systems. Graduate Studies in Mathematics, vol. 140. American Mathematical Society, Providence (2012). MR2961944
36. Tuckwell, H.C., Le Corfec, E.: A stochastic model for early HIV-1 population dynamics. J. Theor. Biol. **195**, 451–463 (1998)
37. Tuckwell, H.C., Shipman, P.D.: Predicting the probability of persistence of HIV infection with the standard model. J. Biol. Syst. **19**(4), 747–762 (2011). doi:10.1142/S0218339011004147. MR2870478
38. Tuckwell, H.C., Wan, F.Y.M.: Nature of equilibria and effects of drug treatments in some simple viral population dynamical models. IMA J. Math. Appl. Med. Biol. **17**, 311–327 (2000)